Supplementary Information

Statistical Variability Analysis of Resistive Switching in Lead-Free Double Perovskite Flexible Memristors

Susmita Das[1], Prabir Kumar Haldar[1], Pranab Kumar Sarkar [2]*

[1]Department of Physics, Cooch Behar Panchanan Barma University, Cooch Behar 736101, India

[2]Department of Applied Science and Humanities, Assam University, Silchar 788011, Assam, India

Corresponding author email: pranab.sarkar83@gmail.com , pranab.kumar.sarkar@aus.ac.in

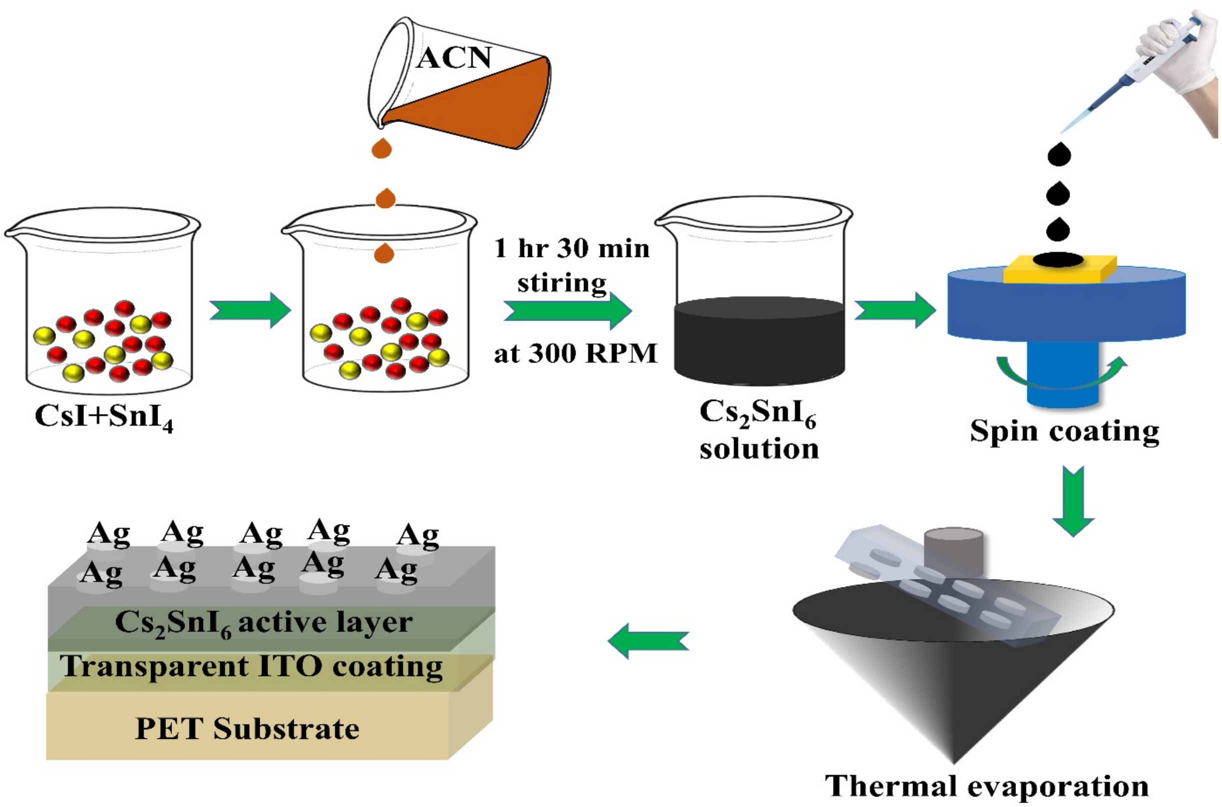

Fig. S1. Schematic diagram of step wise double halide perovskite based thin film device fabrication and top electrode deposition.

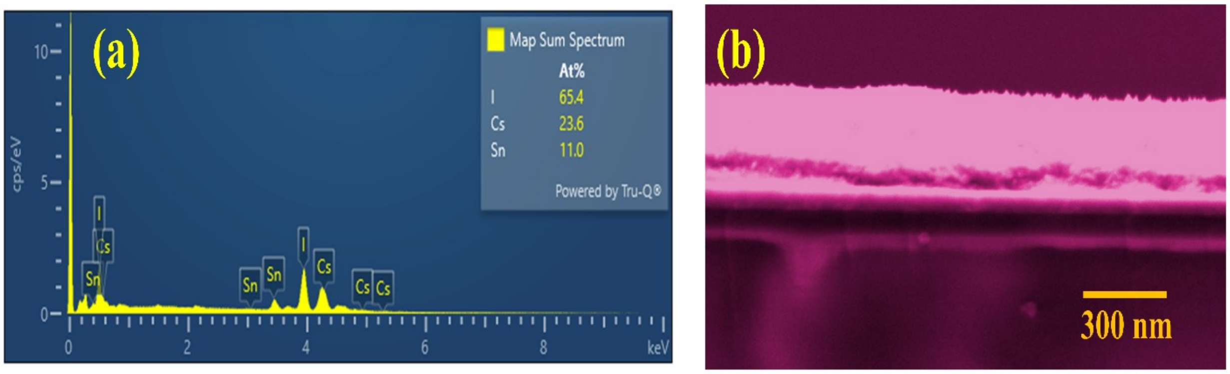

Fig. S2. (a) EDX profile and (b) cross-sectional FESEM image of Cs_2SnI_6 perovskite sample.

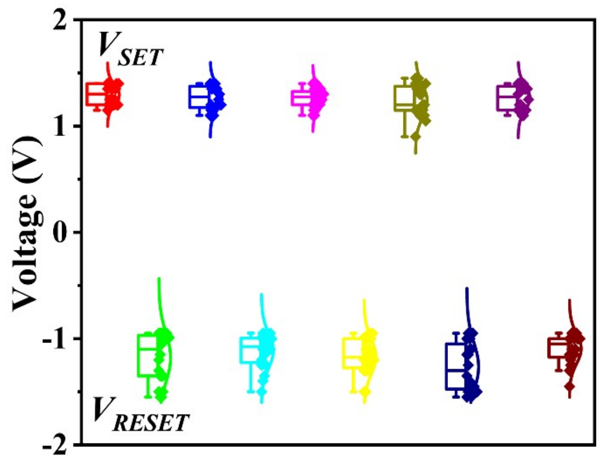

Fig. S3. The batch-to-batch comparison for C/C operation takes 20 cycles per batch

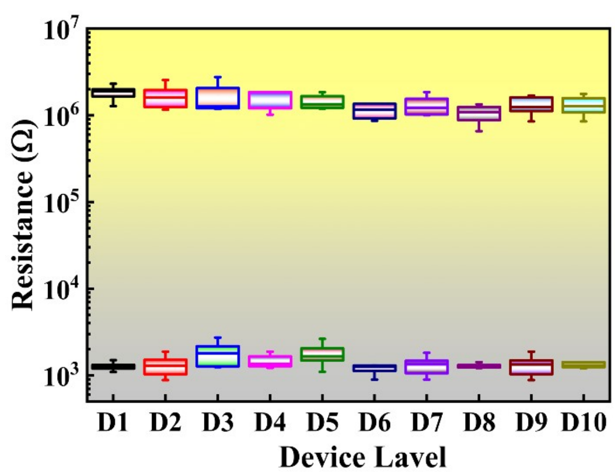

Fig. S4. The LRS HRS distribution of 10 different devices.

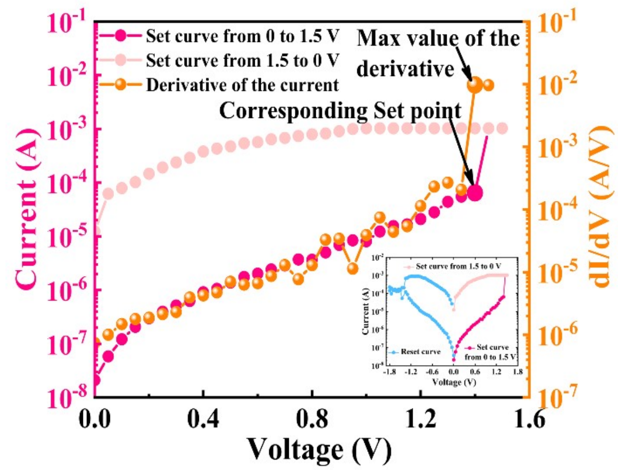

Fig. S5. Experimental current versus voltage curve for a set process corresponding to an Ag/Cs_2SnI_6/ITO device (pink circles). The value of the derivative (orange circles) in the first part of the I-V curve (dark pink), i.e., from 0 to 1.5 V, was calculated to determine the set point by detecting the maximum derivative value. The inset shows a complete I-V cycle including both set and reset processes, to clarify which part of the curve is being analyzed.

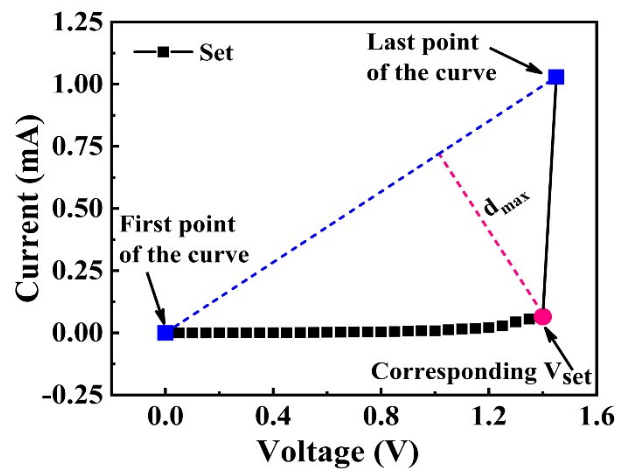

Fig. S6. Experimental current versus voltage curve for a set process corresponding to Ag/Cs_2SnI_6/ITO device. The set point has been established by determining the maximum distance from a straight line that joins the first and last points of the experimental curve.

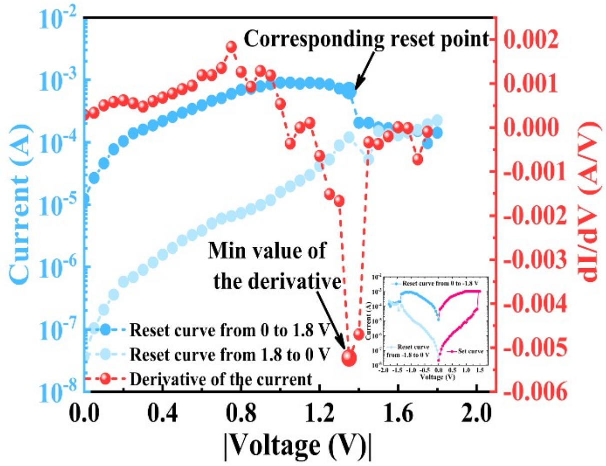

Fig. S7. Experimental current versus voltage curve for a reset process corresponding to an Ag/Cs_2SnI_6/ITO device (sky circles). The value of the derivative has been calculated (red circles) in the first part of the I-V curve (dark sky); i.e., from 0 to 1.8 V to determine the reset point, by detecting the minimum derivative value. The inset shows a complete I-V cycle including both set and reset processes, to clarify which part of the curve is being analyzed.

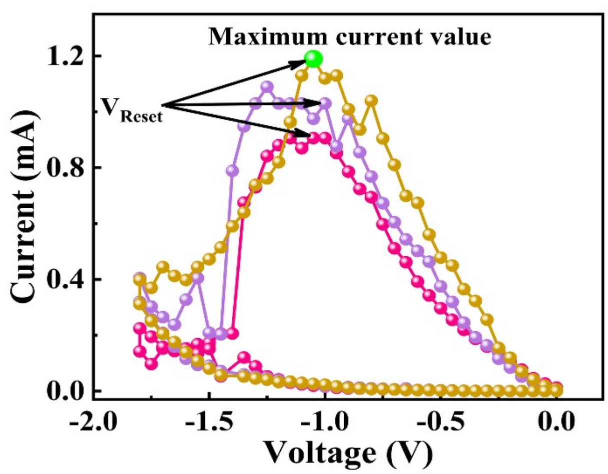

Fig. S8. Experimental current versus voltage curves for three reset processes measured in Ag/Cs_2SnI_6/ITO devices. The reset point in MR3 is established by assuming the maximum value of the current in all the voltage intervals considered.

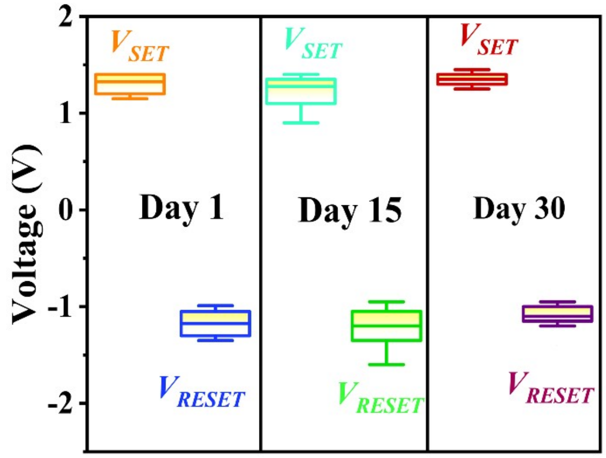

Fig. S9. Statistical distribution of SET and RESET voltages for D/D operation for long-term stability

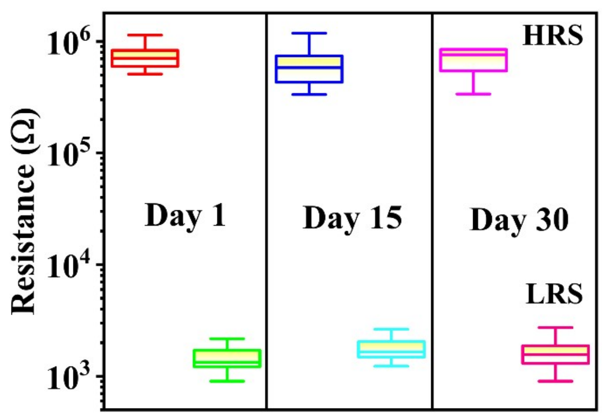

Fig. S10. Statistical distribution of HRS and LRS currents for D/D operation for long-term stability.

Table1 Performance comparison of this work with existing literature studies based on lead-free perovskite memristors

Device Structure	SET/RESET (V)	Filament type and Flexibility	On/ Off ratio	Retention time (s)	Endurance Cycles	Ref
Ag/NiO_x/$Cs_2AgBiBr_6$/SnO_2/ITO	+0.3 to 0.4/−0.3	Vacancy, No bending	50	10^3	3×10^2	1
Ag/Al_2O_3/Cs-Cu-I/ITO Glass	+0.74 to 0.76/−0.4	I vacancies, No bending	>10^3	4×10^3	150	2
Ag/K_2CuBr_3/ITO Glass	0.317/ −0.289	Metal	10^5	10^3	200	3
Ag/PMMA/$CsCu_2I_3$/ITO	+0.5/−0.5	Vacancy	10^4	10^4	100	4

Al/$Cs_2AgBiBr_6$/ITO	−0.5/+1.1	Br Vacancies	10^3	10^4	2×10^3	[5]
Au/$Cs_2AgBiBr_6$/ITO Glass	+0.52/−0.35	Br Vacancies	10^3	10^4	-	[6]
Al/$(Cs_{0.9}Rb_{0.1})_2AgBiBr_6$/ITO	−1.2/+2.8	Br Vacancies, mechanically robust	10^4	10^3	1×10^3	[7]
Ag/$CsSnCl_3$/ITO PET	+0.9/−1.1	Metal, Bending	10^2	10^4	100	[8]
Au/$CsSnBr_3$/ITO Glass	+1.8/−1.46	Vacancy	10^5	10^3	400	[9]
Ag/$CsSnI_3$/Pt/Si/SiO_2	+0.15/−0.1	Metal, vacancy, PMMA	10^3	10^3	600	[10]
Ag/PMMA/$Cs_2AgBiBr_6$/ITO	+1.53/−3.40	Vacancy, Flexible	10	10^5	10^3	[11]
Al/Cs_2NaBiI_6/ITO Glass	−0.3/+2.3	Vacancy high temperature	10^2	10^4	200	[12]
W/$Cs_3Bi_2Br_9$/ITO	+0.53/−0.83	Vacancy, Robust switching endurance	10	10^3	1100	[13]
Ag/$Cs_3Bi_2I_9$/FTO Glass	−0.12/+1	Vacancy	10^6	10^2	250	[14]
Ag/$Cs_3Bi_{2-x}Li_xI_{9-2x}$ (CBL_xI)/ITO (x=0.4)	−0.10/+0.23	Metal	10^2	10^4	128	[15]
Al/$Cs_3Sb_2Cl_9$/ITO	+0.11/−0.56	Cl vacancy	10^2	10^4	750	[16]
Al/$Cs_3Sb_2Br_9$/ITO	+0.32/−0.98	Br vacancy	30	10^4	750	[16]
Al/$Cs_3Sb_2I_9$/ITO	+0.67/−1.07	I vacancy	10	10^4	750	[16]
Al /$Cs_3Sb_2I_9$/ ITO	+0.39/−2.91	Vacancy	10^4	10^4	100	[17]
Al/$Cs_3Cu_2I_5$/ ITO Glass	−0.46/+0.32	Vacancy, No bending	65	10^4	200	[18]
Ag/PMMA/$Cs_3Cu_2I_5$/ ITO	+0.6/−0.44	Metal, vacancy	$\sim10^2$	$>10^4$	100	[19]
Ag/Cs_2SnI_6/ITO-PET	−0.72/+2.87	Vacancy, Flexible with bending stability	$\sim10^3$	10^4	>100	[20]
Ag/Cs_2SnI_6/ITO Glass	−0.82/+1.94	Vacancy, No bending	10^3	10^4	>300	[20]
Ag/Cs_2SnI_6/ITO PET	+1.26/−1.16	Vacancy, Bending stability	10^3	10^4	$>10^6$	This work

References:

1 S. Zhai, J. Gong, Y. Feng, Z. Que, W. Mao, X. He, Y. Xie, X. Li and L. Chu, *iScience*, 2023, **26**, 106461.
2 S. Dutta, S. Panchanan, J. H. Yoo, S. Kumar, H. C. Yoo, S. I. Seok, G. Dastgeer and D. H. Yoon, *Adv Funct Materials*, 2024, **34**, 2410810.
3 Z. Feng, J. Kim, J. Min, P. Guan, S. Zhang, X. Guan, T. Mei, T. Huang, C. Lin, L. Hu, F. Chen, Z. Li, J. Yi, T. Wu and D. Chu, *Adv Elect Materials*, 2025, **11**, 2400804.
4 F. Huang, S. Ge, R. Wei, J. He, X. Ma, J. Tao, Q. Lu, X. Mo, C. Wang and C. Pan, *ACS Appl. Mater. Interfaces*, 2022, **14**, 43474–43481.
5 J. Tang, X. Pan, X. Chen, B. Jiang, X. Li, J. Pan, H. Qu, Z. Huang, P. Wang, J. Duan, G. Ma, H. Wan, L. Tao, J. Zhang and H. Wang, *Adv Funct Materials*, 2025, **35**, 2412375.
6 M. Huang, M. Hou, H. Xing, J. Tu and S. Jia, *Ceramics International*, 2023, **49**, 10365–10374.
7 S. Poddar, S. Mondal, S. Bhattacharjee, P. K. Sarkar, B. K. Das and K. K. Chattopadhyay, *ACS Appl. Mater. Interfaces*, 2025, **17**, 29884–29900.
8 A. Siddik, P. K. Haldar, T. Paul, U. Das, A. Barman, A. Roy and P. K. Sarkar, *Nanoscale*, 2021, **13**, 8864–8874.
9 R. Ray and S. K. Pal, *IEEE Electron Device Lett.*, 2021, **42**, 1284–1287.
10 J. S. Han, Q. V. Le, J. Choi, H. Kim, S. G. Kim, K. Hong, C. W. Moon, T. L. Kim, S. Y. Kim and H. W. Jang, *ACS Appl. Mater. Interfaces*, 2019, **11**, 8155–8163.
11 J. Lao, W. Xu, C. Jiang, N. Zhong, B. Tian, H. Lin, C. Luo, J. Travas-sejdic, H. Peng and C.-G. Duan, *J. Mater. Chem. C*, 2021, **9**, 5706–5712.
12 Y. Zheng, F. Luo, L. Ruan, J. Tong, L. Yan, C. Sun and X. Zhang, *Journal of Alloys and Compounds*, 2022, **909**, 164613.
13 J. Liu, Y. Nie, X. Zhou, J. Qi, D. Li, J. Luo and K. Wang, *J. Mater. Chem. C*, 2025, **13**, 8084–8094.
14 S. Ge, X. Guan, Y. Wang, C. Lin, Y. Cui, Y. Huang, X. Zhang, R. Zhang, X. Yang and T. Wu, *Adv Funct Materials*, 2020, **30**, 2002110.
15 J. Gao, Q. Gao, J. Huang, X. Feng, X. Geng, H. Li, G. Wang, B. Liang, X. Chen, Y. Su, M. Wang, Z. Xiao, P. K. Chu and A. Huang, *ACS Appl. Nano Mater.*, 2023, **6**, 7975–7983.
16 F. Luo, Y. Wu, J. Tong, D. Xu, G. Qin, F. Tian and X. Zhang, *Sci. China Technol. Sci.*, 2023, **66**, 1141–1151.
17 S. Paramanik, A. Maiti, S. Chatterjee and A. J. Pal, *Adv Elect Materials*, 2022, **8**, 2100237.
18 F. Zeng, Y. Tan, W. Hu, X. Tang, Z. Luo, Q. Huang, Y. Guo, X. Zhang, H. Yin, J. Feng, X. Zhao and B. Yang, *J. Phys. Chem. Lett.*, 2021, **12**, 1973–1978.
19 F. Zeng, Y. Guo, W. Hu, Y. Tan, X. Zhang, J. Feng and X. Tang, *ACS Appl. Mater. Interfaces*, 2020, **12**, 23094–23101.
20 A. Kumar, M. Krishnaiah, J. Park, D. Mishra, B. Dash, H. Jo, G. Lee, S. Youn, H. Kim and S. H. Jin, *Adv Funct Materials*, 2024, **34**, 2310780.